CHAPTER IV
POLY(P-PHENYLENE VINYLENE)/ZEOLITE Y COMPOSITES AS A KETONE VAPORS SENSOR: EFFECT OF ALKALINE CATIONS

4.1 Abstract

This work was an attempt to improve the selectivity and sensitivity response of zeolite Y towards three different types of ketone vapors (acetone, MEK, and MIBK) known to be toxic and flammable substances. The effects of cation type, cation concentration, ketone vapor type. and cyclic interval were investigated. Three different cations were exchanged in zeolite Y at 50% mole: NaY; 50KNaY; 50MgNaY; and 50CaNaY for the zeolite Y at fixed Si/Al ratio of 5.1. 50KNaY sample exhibited the highest electrical conductivity sensitivity. This arises from the electrostatic interaction between the cation and the zeolite framework, which affected the adsorption properties of zeolite. The dPPV was mixed with 80KNaY matrix at 10% v/v and was exposed to three different ketone vapors. The highest electrical conductivity sensitivity belonged to the acetone exposure, whereas the MIBK exposure showed the lowest value, as a result of the smaller acetone size. The sensitivity of the composite was higher than that of pure zeolite Y by an order magnitude. For the cyclic interval, the electrical conductivity response decreased with increasing number of the interval due to the interaction between the active site and ketone vapors. The response of samples was irreversible as evidenced by FTIR.

Keywords: Poly(p-Phenylene Vinylene), 2-Propanone (Acetone), Butan-2-one (MEK), 4-Methylpentan-2-one (MIBK), and Zeolite Y

4.2 Introduction

The development of gas sensing materials with selectivity and reliability for volatile organic compounds (VOCs) detection has been of interest in many industrial process controls to control the pollution. Many industrial processes such as utilized ketone group solvents: acetone (2-propanone); MEK (butan-2-one); MIBK (4-

methylpenta-2-one); xylene; toluene; and alcohol (methanol, ethanol, and propanol) which are known to be flammable, toxic, and harmful to human (Heeger *et al.*, 1998; Jung *et al.*, 2008; Tang *et al.*, 2008; Vijaya *et al.*, 2008; Mori *et al.*, 2009; Gao *et al.*, 2011).

One of the possible sensor modes is the electrical conductivity response when exposed to volatile organic compounds vapors human (Heeger *et al.*, 1998; Ruangchuay *et al.*, 2004; Montserral *et al.*, 2007; Jung *et al.*, 2008; Wannatong *et al.*, 2008; Tang *et al.*, 2008; Vijaya *et al.*, 2008; Benvenho *et al.*, 2009; Li *et al.*, 2009; Mori *et al.*, 2009; Thongchai *et al.*, 2009; Gao *et al.*, 2011). Various types of material are used as gas sensors: conductive polymers (Jung *et al.*, 2008; Benvenho *et al.*, 2009; Li *et al.*, 2009); porous materials (Jalkane *et al.*, 2010; Chang *et al.*, 2011); and metal oxides (Chang *et al.*, 2010; Hung *et al.*, 2012). Zeolites are porous material which has been widely used as a gas sensing material such as faujasite (zeolite x and zeolite Y), ZSM-5, and mordenite (MOR). Zeolite has a high thermal stability, good chemical resistance, high porosity, high surface area, and good selective and adsorption properties towards particular gases and vapors. These characteristic properties of zeolite have been explored and utilized towards gas sensing (Gao *et al.*, 2011; Yang *et al.*, 2007; Li *et al.*, 2010; Varsani *et al.*, 2011; Yimlamai *et al.*, 2011). However, the electrical conductivity of zeolite is rather low. There have been several methods to improve the electrical conductivity and the electrical conductivity sensitivity properties of zeolite such as the ion exchange process, the reduction in the Al content in the zeolite structure, and the blending with other conductive polymers (Gao *et al.*, 2011; Ruangchuay *et al.*, 2004; Ruangchuay *et al.*, 2008; Thongchai *et al.*, 2009). The alkaline and alkaline earth cations are the one of the factors control the electrical conductivity and the adsorption properties. Recently, the exchange process and the mixing of a conductive polymer into a zeolite matrix has been attempted to improve of electrical conductivity of zeolite as a sensing materials to detect toxic gases (Ahlskog *et al.*, 1997; Heeger *et al.*, 1998; Ruangchuay *et al.*, 2004; Montserral *et al.*, 2007; Thuwachaosoan *et al.*, 2007; Jung *et al.*, 2008; Wannatong *et al.*, 2008; Tang *et al.*, 2008; Vijaya *et al.*, 2008; Benvenho *et al.*, 2009; Li *et al.*, 2009; Mori *et al.*, 2009; Thongchai *et al.*, 2009; Kamonsawas *et al.*, 2010; Gao *et al.*, 2011).

Poly(p-phenlene vinylene) (PPV) is the one of conductive polymers that has been widely used in gas sensing applications because it has high electrical conductivity after doping with sulfuric acid, good mechanical properties, good chemical stability, and is easy to synthesize (wessling *et al.*, 1968; McKeen *et al.*, 2009). Doped PPV or dPPV may have a positive or negative response depending on the electrophilic or nucleophilic nature of the gases or chemical vapors. But PPV itself generally has poor selective and adsorption properties towards particular gases and chemical vapors. Therefore, combining the good characteristics of zeolite and the conductive polymer is expected to improve the selective, adsorptive, and electrical conductivity properties by mixing the conductive PPV into the zeolite matrix (Thuwachaosoan *et al.*, 2007; Jalkane *et al.*, 2010).

In this work, the effects of the cation type and the cation concentration of zeolite Y, at the fixed Si/Al ratio of 5.1, on the electrical conductivity sensitivity towards an acetone vapor are investigated. Then, the electrical conductivity response of the dPPV and zeolite Y composite towards the three different types of ketone vapor sensors (acetone, MEK, and MIBK) are also investigated.

4.3 Experimental

4.3.1 Materials Preparation

4.3.1.1 Synthesis of Poly(p-phenylene vinylene) or PPV and Doping Process

PPV was chemically synthesized with α, α'-dichloro-p-xylene (Aldrich) and tetrahydrothiophene (Aldrich) to form a p-xylene-bis(tetrahydrothiophenium chloride) monomer. The sodium hydroxide induced the polymerization of the p-xylene-bis(tetrahydrothiophenium chloride) monomer to form a precursor polymer and PPV was essentially obtained by heating the precursor polymer under vacuum at 180 °C for 6 h (Wessling *et al.*, 1968). The doping process occurred after adding the 18 M sulfuric acid solution at the mole ratio of 1:100 (PPV repeating uints and sulfuric acid) to the polymer powder. The process was monitored by observing the change of polymer color from bright yellow to black brown (Wessling *et al.*, 1968).

4.3.1.2 The Cation Exchange Process

The zeolite Y (Si/Al=5.1 and Na^+) or NaY was purchased from Zeolyst. The NaY with different cation types were obtained by an ion exchange process. The solution of $MgCl_2$, $CaCl_2$, and KCl at 1.0 M was added in to 5 grams of NaY and strired at 25 °C for 24 h to prepare zeolite Y (Si/Al=5.1, 50% mole of Na^+, and 50% mole of Mg^{2+}) or 50MgNaY, zeolite Y (Si/Al=5.1, 50% mole of Na^+, and 50% mole of Ca^{2+}) or 50CaNaY, zeolite Y (Si/Al=5.1, 70% mole of Na^+, and 30% mole of K^+) or 30KNaY, zeolite Y (Si/Al=5.1, 50% mole of Na^+, and 50% mole of K^+) or 50KNaY, and zeolite Y (Si/Al=5.1, 20% mole of Na^+, and 80% mole of K^+) or 80KNaY. Then zeolite samples were filtered and washed with DI-water for 5 times (Scott *et al.*, 2003; Li *et al.*, 2010).

4.3.1.3 Preparation of dPPV_Zeolilte Y Pellet

The zeolite Y: NaY; 50MgNaY; 50CaNaY; 30KNaY; 50KNaY; and 80KNaY at the same Si/Al ratio (5.1) were used as the matrices. The dPPV_zeolite Y composites were prepared by a dry random mixing the zeolite Y with dPPV particles at 10% v/v of dPPV. The composites were compressed into a disc form by using a hydraulic press at the pressure of 6 kN.

4.3.2 Characterization of PPV, dPPV and Composite

An FT-IR spectrometer (Inclolet, model FRA 106/S) was used to characterize functional groups of PPV, dPPV, and the interaction between the ketone vapors and the active site on the gas sensing materials. A scanning electron microscope (SEM, Hitachi, model S4800) was used to study the morphology of PPV, dPPV, zeolite Y, the 10% v/v of dPPV on the composites or dPPV_[90]80KNaY, and the dispersion of the conductive polymer particles in zeolite Y, at the magnifications of 1000x and 5000x and at 5 and 10 kV. The surface area analysis (Sorptomatic-1990) was used to measure the pore sizes and the surface areas of the zeolite Y. The amount of cation was determined by an atomic adsorption spectrophotometer (Varian, Spectra A300). A custom made two-point probe with a linear geometric array and connected with a voltage supplier (Keithley, 6517A) was used to measure the specific electrical conductivity.

4.3.3 Electrical Conductivity and Chemical Vapor Detection

The electrical conductivity values of the gas sensing pellets under exposures to air, N_2, and chemical vapors were measured by using the custom made two-point probe, in the chemical chamber connected to a voltage supplier (Keithley, 6517A) in which its voltage was varied and the resultant of current was measured. The electrical conductivity was calculated by utilizing the equation 4.1.

$$\sigma = (I/KVt) \qquad 4.1$$

where I is the measured current (A), V is the applied voltage (V), t is the thickness, and K is the geometric correction factor of the two-point probe, as determined by calibrating the probe with a silicon wafer possessing a known resistivity value.

For the chemical vapor detection, the chemicals were used in this work were acetone, MEK, and MIBK (Labscan, AR grade). All of ketone vapors were prepared through a flow system at the vapor concentration of 30000 ppm (3% v/v) in N_2. Nitrogen (N_2, TIG) was used as the surface cleaning gas and to vaporize the chemical solvents. All chemicals were used without further purifications. The detection system is as shown in Figure 4.1. For the cyclic interval investigation, the measurement is 1200 sec for each cyclic interval. And each cyclic internal was evacuated of air and moisture by using a vacuum pump until steady state was obtained. N_2 gas was injected into the chamber and the steady state electrical conductivity was recorded as $\sigma_{N2,\text{before exposure}}$. Then chamber was evacuated before injecting the chemical vapor into the chamber. The ketone vapor was injected into the chamber and the steady state electrical conductivity was recorded as $\sigma_{\text{chemical vapor}}$. The ketone vapor was removed by the vacuum pump and N_2 was injetced into the chamber. and the electrical conductivity was measured as $\sigma_{N2,\text{ after exposure}}$. The electrical conductivity response and sensitivity of the composites were determined by following the equation 4.2 and 4.3.

$$\Delta\sigma = \sigma_{\text{chemical vapor}} - \sigma_{N2,\text{ before exposure}} \qquad 4.2$$

$$\text{Sensitivity} = \Delta\sigma / \sigma_{N2\text{ before exposure}} \qquad 4.3$$

$\Delta\sigma$ is the difference in the specific electrical conductivity (S/cm). where $\sigma_{N2,\text{ before exposure}}$ is the specific electrical conductivity in N_2 before exposure (S/cm), and $\sigma_{\text{chemical vapor}}$ is the specific electrical conductivity under chemical vapor exposure

(S/cm) (Soontornworajit *et al.*, 2007; Thuwachaosoan *et al.*, 2007; Kamonsawas *et al.*, 2010).

4.4 Results and Discussion

4.4.1 Characterization of dPPV, Zeolite Y and Composites

The main analytical data and the electrical conductivity data in air and N_2 of dPPV, zeolite Y with different cations but the same Si/Al ratio (5.1), and the composites are tabulated in Table 4.1. The molecular structures of acetone, MEK and MIBK are shown in Figure 4.2. The SEM morphology of dPPV, 80KNaY, and dPPV_[90]80KNaY are shown in Figure 4.3.

The cage size of zeolite Y (Si/Al=5.1 and Na^+) or NaY is 1.3 nm and connected with a 0.74 nm window ((Florian *et al.*, 1994). Figure 2 shows the molecular structure of three different types of ketone: acetone (2a), MEK (2b), and MIBK (2c) with length scales of 0.524 nm, 0.677 nm, and 0.828 nm, respectively. It is anticipated that the acetone and MEK molecules can penetrate to the zeolite Y framework. However, the MIBK molecule is larger than the zeolite Y cage, and it is not expected to penetrate into the zeolite Y cage (Florian *et al.*, 1994; Li *et al.*, 2010).

The amounts of K^+, Mg^{2+}, and Ca^{2+} ion exchanged with Na^+ in the zeolite Y were determined by an atomic adsorption spectrophotometer in terms of percentage mole of cation. The %mole of cation exchange is defined as the ratio of K^+, Mg^{2+}, and Ca^{2+} divided by the sum of the moles of the cation and Na^+ multiplied by 100 (Soontornworajit *et al.*, 2007) For the NaY ion exchanged with K^+, the mole percentages are 30, 56, and 81 for the ion exchange times of 3, 12, and 24 h, respectively. For the NaY exchanged with Mg^{2+} and Ca^{2+}, the mole percentages are 53 and 56 for the ion exchange time of 24 h, as listed in Table 4.1.

Figures 4.3a and 4.3b show the SEM monographs of dPPV or doped dPPV, zeolite Y (Si/Al=5.1, K^+ and Na^+) or 80KNaY particles, at the magnification of 1000x, and at 5 kV; they appear to be moderately uniform in shape and sizes. A nearly uniform dispersion of dPPV particles within the zeolite Y matrix pellet and powder can be observed in Figures 4.3c and 4.3d (Ahlskog *et al.*, 1997;

Thuwachaosoan *et al.*, 2007; Wannatong *et al.*, 2008; Thongchai *et al.*, 2009; Kamonsawas *et al.*, 2010).

The electrical conductivity values of 50KNaY, NaY, 50CaNaY, and 50MgNaY and under N_2 condition are 1.06 $\times10^{-03}$ ± 2.27 $\times10^{-04}$ S/cm, 8.38 $\times10^{-04}$ ± 2.27 $\times10^{-05}$ S/cm, 7.69 $\times10^{-04}$ ± 3.70 $\times10^{-06}$ S/cm, and 3.73 $\times10^{-04}$ ± 3.71 $\times10^{-06}$ S/cm, respectively, as tabulated in Table 4.1. For the effects of cation type, the electrical conductivity of 50MgNaY is lower than NaY, 50CaNaY, and 50KNaY, respectively. This is because of the EN of Mg^{2+} (1.31) is higher than Ca^{2+} (1.00), Na^+ (0.93), and K^+ (0.82). The large value of electronegativity and the small size of charge balancing ion lead to reduced proton mobility in the zeolite Y framework (Florian *et al.*, 1994; Auerbach *et al.*, 2003; Li *et al.*, 2010; Yimlamai *et al.*, 2011). The electrical conductivity of dPPV in N_2 condition is 2.21 $\times10^{-02}$ ± 6.21 $\times10^{-04}$ S/cm. When mixing dPPV in the 80KNaY matrix, the electrical conductivity increases up to 5.86 $\times10^{-03}$ ± 2.27 $\times10^{-03}$ S/cm. Thus, dPPV has been shown to improve the electrical conductivity of zeolite Y by an order of pure 80KNaY (Thuwachaosoan *et al.*, 2007; Thongchai *et al.*, 2009). The electrical conductivity sensitivity of dPPV, 50MgNaY, NaY, 50CaNaY, 50KNaY, and dPPV_[90]80KNaY pellets exposed to three different types of ketone vapor is shown and discussed next.

4.4.2 The Response of Zeolite Y at the Cyclic Interval of 1200 sec

4.4.2.1 The Effect of Cation Type

Zeolite Y (Si/Al=5.1 and Na^+) or NaY ion exchanged with Mg^{2+}, Ca^{2+}, and K^+ 50% mole are investigated for the effect of cation types and the cyclic response at the cyclic interval of 1200 sec towards the 3% v/v acetone vapor in N_2. Figure 4.4 shows the plot of electrical conductivity sensitivity of 50MgNaY, 50CaNaY, NaY, and 50KNaY versus cation radius (Å) and electronegativity (EN) towards the acetone vapor at concentration of 3% v/v in N_2. The electrical conductivity sensitivity values in the 1st interval of 50MgNaY, 50CaNaY, NaY, and 50KNaY are 1.97 $\times10^{-01}$ ± 5.06 $\times10^{-03}$, 2.57 $\times10^{-01}$ ± 2.40 $\times10^{-03}$, 2.65 $\times10^{-01}$ ± 1.89 $\times10^{-02}$, and 3.42 $\times10^{-01}$ ± 4.67 $\times10^{-04}$, respectively, as tabulated in Table 4.2. The electrical conductivity sensitivity increase with increasing of cationic radius and decreasing electronegativity (EN), because the large cationic radius corresponds to the reduced electrostatic interaction between the cation and the zeolite framework, resulting in the cation ability to transfer to another cage or the increase in proton mobility (Florian *et al.*, 1994; Auerbach *et al.*, 2003; Kamonsawas *et al.*, 2010; Li *et al.*, 2010; Yimlamai *et al.*, 2011). The cationic radius of K^+ (1.51 Å) is larger than Na^- (1.16 Å), Ca^{2+} (1.14 Å), and Mg^{2+} (0.71 Å), respectively. Therefore, 50KNaY shows the highest electrical conductivity sensitivity value than those of NaY, 50CaNaY, and 50MgNaY when exposed acetone vapor at a concentration of 3% v/v in N_2.

4.4.2.2 The Effect of Cation Concentration

The effect of the cation concentration in zeolite Y after ion exchanged with containing 0, 30, 50, and 80% mole of K^- on the electrical conductivity sensitivity towards the acetone vapor at 3% v/v in N_2 is investigated and shown in Figure 4.5. The electrical conductivity sensitivity values of NaY, 30KNaY, 50KNaY, and 80KNaY in the 1st interval response are $2.65 \times 10^{-01} \pm 1.89 \times 10^{-02}$, $2.78 \times 10^{-01} \pm 4.22 \times 10^{-03}$, $3.42 \times 10^{-01} \pm 4.67 \times 10^{-04}$, and $4.26 \times 10^{-01} \pm 1.25 \times 10^{-04}$ as K^+ concentration in NaY increases from 0, 30, 50, and 80% mole of K^+, respectively. The electrical conductivity sensitivity value increases increasing percentage of K^- in the NaY because of K^+ has a smaller electronegativity (EN) value than Na^+ which leads to the increase in the proton mobility and the ability to interact with acetone vapor more easier. Thus, increasing potassium cation concentration in NaY and exposing to acetone vapor, results in the interaction between active site on the zeolite Y and acetone vapor to become more favorable. For the next interval, the electrical conductivity decreases because the interaction is not reversible and thus the reduced the proton mobility (Biaglow *et al.*, 1993; Florian *et al.*, 1994; Fameth *et al.*, 1995; Jian *et al.*, 1998; Panov *et al.*, 1998; Boekfa *et al.*, 2010; Yimlamai *et al.*, 2011). In this present work, 80KNaY is used to study the effects of dPPV and solvent types next.

4.4.3 The Response of dPPV_90[80]KNaY towards Ketone Vapors

DPPV was mixed into the 80KNaY at 80% mole of K^+ cation making up the 80KNaY matrix with 10% v/v of dPPV or dPPV_[90]80KNaY. The electrical conductivity sensitivity values of the dPPV, dPPV_[90]80KNaY and 80KNaY towards the acetone vapor at 3% v/v in the 1st cyclic interval are 4.50 ± 9.88 x10^{-01}, 4.13 ± 7.09 x10^{-02}, and 4.26 x10^{-01} ± 1.25 x10^{-04}, respectively, as shown in Figure 4.6 and Table 4.2. The highest electrical conductivity sensitivity toward the acetone vapor is dPPV because dPPV has a conjugated double bond which leads to induce the electron transfer along the conductive polymer molecule, resulting in the increase in the electrical conductivity sensitivity towards the acetone vapor (Wessling *et al.*, 1968; Thuwachaosoan *et al.*, 2007; Thongchai *et al.*, 2009). However, 80KNaY can only transfer protons in the zeolite framework, resulting in lower electrical conductivity than dPPV or other conductive polymers (Biaglow *et al.*, 1993; Florian *et al.*, 1994; Fameth *et al.*, 1995; Jian *et al.*, 1998; Panov *et al.*, 1998; Boekfa *et al.*, 2010). Thus, mixing the dPPV in 80KNaY leads to an increase in the electrical conductivity sensitivity by an order magnitude of 80KNaY (Thuwachaosoan *et al.*, 2007; Thongchai *et al.*, 2009). The effect of ketone vapor type is shown and investigated next. Figure 4.6 shows the electrical conductivity response of dPPV_[90]80KNaY exposed to the acetone, MEK, and MIBK vapors, respectively. The electrical conductivity of dPPV_[90]80KNaY in the 1st interval response increases significantly when exposed to acetone vapor in comparison with the exposures to the MEK and MIBK vapors. The electrical conductivity sensitivity of dPPV_ [90]80KNaY towards acetone, MEK, and MIBK are 4.13 ± 7.09 x10^{-02}, 2.17 ± 9.55 x10^{-02}, and 1.01 ± 1.03 x10^{-02}, respectively, as shown in Figure 4.6. The larger response in the 1st interval of dPPV_[90]80KNaY and higher sensitivity value occur towards acetone vapor than MEK and MIBK, respectively. The acetone (0.524 nm) is of a smaller molecular size than MEK (0.667 nm) and MIBK (0.828 nm), resulting in easier penetrate ion in the zeolite framework as compare to MEK and MIBK. Thus, the interaction between dPPV_[90]80KNaY is more favorable when exposed to acetone than in MEK and MIBK. Similar results are obtained in the following interval (2nd, 3rd, and 4th interval), but the electrical conductivity is lower than the previous interval, as shown in Figure 4.9 (Biaglow *et al.*, 1993; Hoost *et al.*, 1996; Ahlskog *et al.*. 1997; Panov *et al.*, 1998; Thuwachaosoan *et al.*, 2007; Wannatong *et al.*, 2008; Thongchai *et al.*, 2009; Kamonsawas *et al.*, 2010; Li *et al.*, 2010; Yimlamai *et al.*, 2011).

4.4.4 The Effect of Cyclic Interval

The 50KNaY, NaY, 50CaNaY, and 50MgNaY samples are used to investigate the effect of cyclic interval time when exposed to acetone vapor at concentration of 3% v/v in N_2. The electrical conductivity sensitivity values of 50KNaY in the 1st, 2nd, 3rd, and 4th interval are $3.42\text{x}10^{-01} \pm 4.67\ \text{x}10^{-04}$, $2.09\ \text{x}10^{-01} \pm 6.27\ \text{x}10^{-04}$, $1.81\ \text{x}10^{-01} \pm 6.12\ \text{x}10^{-04}$, and $1.28\ \text{x}10^{-01} \pm 9.12\ \text{x}10^{-04}$, respectively, as shown in Figure 4.7a (top) and tabulated in Table 4.2. The electrical conductivity sensitivity decreases with an increasing number of cyclic interval because of the interactions from the previous interval are not reversible leading to a reduced number of active sites and proton mobility with zeolite Y. Similar results are obtained in the other cations as well (NaY, 50CaNaY, and 50MgNaY) (Biaglow *et al.*, 1993; Florian *et al.*, 1994; Panov *et al.*, 1998; Yimlamai *et al.*, 2011).

The cyclic interval of dPPV_[90]80KNaY towards three different ketone vapors (acetone, MEK, and MIBK) at a concentration of 3% v/v in N_2 is investigated next. The electrical conductivity sensitivity of dPPV_[90]80KNaY towards the acetone vapor at the 1st, 2nd, 3rd, and 4th are $4.13 \pm 7.09\ \text{x}10^{-02}$, $1.43 \pm 1.61\ \text{x}10^{-02}$, $9.10\ \text{x}10^{-01} \pm 6.98\ \text{x}10^{-03}$, and $5.27\ \text{x}10^{-01} \pm 2.68\text{x}10^{-03}$, respectively, as shown in Figure 4.7b (bottom) and listed in Table 4.2. The electrical conductivity sensitivity decreases with increasing numbers of cyclic intervals. The interaction is not completely reversible for 80KNaY, and the interaction between dPPV and acetone vapor is an irreversible one. Thus, mixing the 10% v/v of dPPV in 80KNaY matrix leads to the irreversible interaction of the composite system and reduced active sites for the next interval (Thuwachaosoan *et al.*, 2007; Thongchai *et al.*, 2009; Yimlamai *et al.*, 2011). Similar results are obtained in the MEK and MIBK exposures.

4.4.5 FTIR Investigations of Reactions of Adsorbed Acetone Vapor

The interaction between zeolite Y and the ketone vapor is discussed from FTIR spectrum. The FTIR spectra of 80KNaY and dPPV_[90]80KNaY were taken in the 650-4000 cm^{-1} regions (Figures 4.8 and 4.9). The spectra were collected before (a), during exposure (1st interval) (b), during exposure (2nd interval) (c), during exposure (3rd interval) (d), and after the acetone exposure (e).

Figure 4.8 shows the FTIR spectra of 80KNaY before (4.8a), during acetone exposure 15 min interval (4.8b), and after the acetone exposure (4.8e). Before acetone exposure, the adsorption of the Si-OH group (ν =3630 cm^{-1}) can be assigned to the zeolite characteristics (Biaglow *et al.*, 1993; Panov *et al.*, 1998; Li *et al.*, 2010; Yimlamai *et al.*, 2011). The peaks at 790 and 1010 cm^{-1} are the characteristics of the tetrahedral unit (Panov *et al.*, 1998). A peak at 1640 cm^{-1} is the OH stretching which suggests the possibility of water in the zeolite structure (Soontornworajit *et al.*, 2007; Wannatong *et al.*, 2008; Li *et al.*, 2010; Yimlamai *et al.*, 2011). During acetone exposure, the spectrum shows new peaks at 3420, 1715, and 1210 cm^{-1}; the former can be assigned to the interaction between oxygen on the carbonyl group and the potassium cation in the zeolite framework, as shown in Figure 10a. The new peak at 3420 cm^{-1} is assigned to the interaction between oxygen on the carbonyl group and hydrogen in the zeolite (Florian *et al.*, 1994; Panov *et al.*, 1998; Hoost *et al.*, 1996; Boekfa *et al.*, 2010; Li *et al.*, 2010; Yimlamai *et al.*, 2011). After exposure to acetone in the 2nd and 3rd intervals, the interaction between the active sites and acetone molecule diminishes. Moreover, the responses in the 2nd and 3rd intervals are lower than the 1st interval, because the interaction is not reversible. This confirms that there are some residue interactions remaining between the acetone and 80KNaY from the previous interval, resulting in lower electrical conductivity response towards acetone in the next intervals. When replaced with nitrogen (4.8e), the IR spectrum peaks at 3420 and 1210 cm^{-1} evidently decrease; this also confirms that the interaction between acetone and the 80KNaY is not reversible, suggesting the irreversible responses to acetone under repeated exposures (Soontornworajit *et al.*, 2007; Thuwachaosoan *et al.*, 2007; Kamonsawas *et al.*, 2010; Li *et al.*, 2010; Yimlamai *et al.*, 2011).

Figure 4.9 shows the corresponding IR spectra of dPPV_[90]80KNaY. Before the acetone exposure, the adsorption peak of the quinoid structure, a characteristic of dPPV, appears at ν = 1140 cm^{-1}. The characteristics of phenylene are the peaks at 1520, 2960, and 3022 cm^{-1} (Wessling *et al.*, 1968; Thongchai *et al.*, 2009; Kamonsawas *et al.*, 2010). The peak at around 3630 cm^{-1} is assigned to the Si-OH group (Florian *et al.*, 1994; Panov *et al.*, 1998; Hoost *et al.*, 1996; Li *et al.*, 2010; Yimlamai *et al.*, 2011). During the acetone exposure, in the 1st cycle, the new peaks at 3449 and 1210 cm^{-1} are the interaction between acetone and 80KNaY (Florian *et al.*, 1994; Panov *et al.*, 1998; Hoost *et al.*, 1996; Li *et al.*, 2010; Yimlamai *et al.*, 2011). The new peak at 1380 cm^{-1} indicates the C-O stretching; this also suggests an interaction between acetone and dPPV, as shown in Figure 4.10b. The increase in the intensity at 1140 cm^{-1} during the acetone exposure is caused by the increase in the number of the quinoid structure of dPPV (Wessling *et al.*, 1968; Thongchai *et al.*, 2009; Kamonsawas *et al.*, 2010). After an evacuation and exposures to the acetone vapor in the 2nd and 3rd intervals, the interaction still remains, causing the lower electrical conductivity response than the previous interval, a similar result to 80KNaY. After the acetone exposure, the intensities at 3022, 2960, and 1520 cm^{-1} decrease; these suggesting that acetone may act as a secondary dopant to increase the number of the quinoid structures in the dPPV chain (Wessling *et al.*, 1968; Thongchai *et al.*, 2009; Kamonsawas *et al.*, 2010). The interaction is clearly irreversible.

Figure 4.10a shows the interaction of 80KNaY with acetone vapor. Acetone is an electron donating molecule which stabilizes the potassium cation in the 80KNaY structure. Thus, an electron from the acetone can move along the 80KNaY structure easily and thus the increase in the electrical conductivity when exposed to acetone vapor (Fameth *et al.*, 1995; Panov *et al.*, 1998; Yimlamai *et al.*, 2011). When dPPV is mixed with 80KNaY matrix at 10% v/v and exposed to acetone vapor, acetone acts as an electron donating species for the 80KNaY and dPPV structures as shown in Figure 4.10b. The lone pair electron from carbonyl of the acetone molecule stabilizes the cation on the dPPV chain resulting in greater negative charges along the dPPV molecule, and corresponding to higher electrical conductivity when exposed to acetone vapor (Thongchai *et al.*, 2009; Kamonsawas *et al.*, 2010).

4.5 Conclusions

The NaY (Si/Al=5.1) was successfully ion exchanged into KNaY at 30, 50, and 80% moles of the cation, MgNaY at 50% mole of the cation, and CaNaY at 50% mole of the cation. These ion exchanged zeolites was used to investigate the effects of cation type, cation concentration, solvent type, and the cyclic interval on the electrical conductivity response towards ketone vapors at 3% v/v in N_2. The 50KNaY sample showed the highest electrical conductivity when compared with NaY, 50CaNaY, and 50MgNaY towards acetone vapor, due to the proton mobility in the zeolite framework. Increasing the cation size in the zeolite framework led to the reduced electrostatic interaction between the zeolite framework and the cation, and to the ease in which a proton can transfer. For the effect of cation concentration, 80KNaY exhibited the highest electrical conductivity, whereas 30KNaY showed the lowest value which was comparable in magnitude to that of NaY. dPPV was mixed into the 80KNaY matrix and exposed to three different ketone vapors (acetone, MEK, and MIBK) at 3% v/v in N_2. The acetone exposure provided the highest electrical conductivity sensitivity, whereas MIBK showed the lowest value due to the ability of the acetone molecule to penetrate into the zeolite framework. Thus, the electrical conductivity sensitivity was shown to be enhanced by mixing dPPV into the 80KNaY matrix. For the cyclic interval, the electrical conductivity response decreased with increasing number of cyclic intervals towards the acetone vapor, due to the irreversible interaction between the zeolite and the acetone vapor. The irreversible interactions between the active site and the ketone vapors were irreversible as evidenced by the FTIR spectrum.

4.6 Acknowledgements

The author would like to acknowledge the financial support from: The Conductive and Electroactive Polymers Research Unit of Chulalongkorn University; The Thailand Research Fund (TRF-RTA, TRF-RGJ PHD/0026/2553); and The Royal Thai Government.

4.7 References

Ahlskog, M., Reghu, M., Noguchi, T., and Ohnishi, T. (1997) Doping and conductivity studies poly(p-phenylene vinylene). Synthetic Metals, 89, 11-15.

Auerbach, S.M., Carrado, K.A., and Dutta, P.K. (Eds.) (2003) Handbook of Zeolite Science and Technology. New York: Marcel Dekker.

Benvenho, A.R.V., Li, R.W.C., and Gruber, J. (2009) Polymeric electronic gas sensor for determining alcohol content in automotive fuels. Sensors and Actuators B: Chemical, 136, 173-176.

Boekfa, B., Pantu, P., Prosbt M., and Limtrakul, J. (2010) Adsorption and tautomerization reaction of acetone on acidic zeolites: the confinement effect in different types of zeolites. Journal of Physical Chemistry C, 114, 15061-15067.

Biaglow, A.I., Gorte, R.J., and David, W. (1993) Molecular motions and 13C chemical shift anisotropy of acetone adsorbed inH-ZSM-5 zeolite. Journal of Physical Chemistry B, 97, 7135-7137.

Chang, J.C., Hung, S.T., Lin, C.K., Chen, C.Y., and Kuo, E.H. (2010) Selective growth of ZnO nanorods for gas sensors using ink-jet printing and hydrothermal processes. Thin Solid Films, 519, 1693-1698.

Chang, C.J., Lin, C.K., Chen, C.C., Chen, Y.C., and Kuo, E.H. (2011) Gas sensor with porous three dimensional framework using TiO_2/polymer double shell hollow microsphere. Thin Solid Films, 520, 1546-1553.

Fameth, W.E. and Gorte. R.J. (1995) Methods for characterizing zeolite acidity. Chemical Reviews, 95, 615-635.

Florian, J. and Kubelkova, L. (1994) Proton transfer between H-Zeolite and adsorbed acetone or acetonitrile: quantum chemical and FTIR study. Journal of Physical Chemistry C, 98, 8734-8741.

Gao, J.F., Yan, D.X., Huang, H.D., Zeng, X.B., Zhang, W.Q., and Li, Z.M. (2011) Tunable positive liquid coefficient of an anisotropically conductive carbon nanotube-polymer composite. Journal of Polymer Research, 18, 2239-2243.

Heeger, A.J. and Diaz-Gracia, M.A. (1998) Semiconducting polymers as a material for photonic device. Current Opinion in Solid State Materials Science, 3, 16-22.

Hoost, T.E., Laframboise, K.A., and Otto, K. (1996) Infrared study of acetone and nitrogen oxides on Cu-ZSM-5. Catalysis Letters, 37, 153-156.

Hung, S.T., Chang, C.J., Hsu, C.H., Chu, B.H., Lo, C.F., Hsu, C.C., Pearton, S.J., and Holzworth, M.R. (2012) SnO_2 functionalized AlGaN/GaN high electron mobility transistor for hydrogen sensing application. International Journal of Hydrogen Energy, 37, 13783-13788.

Jalkane, T., Tuura, J., Makila, E., and Salonen, J. (2010) Electro-optical porous silicon gas sensor with enhance selectivity. Sensors and Actuators B: Chemical, 147, 100-104.

Jung, Y.S., Jung, W., Tuller, H.L., and Ross, C.A. (2008) Nanowire conductive polymer gas sensor patterned using self-assembled block copolymer lithography. Nano Letters, 8, 3776-3780.

Kamonsawas, J., Sirivat, A., Niamlang, S., Hormnirun, P., and Prissanaroon-Ouijai, W. (2010) Electrical conductivity response of poly(phenylene vinylene)/ zeolite composites exposed to ammonium nitrate. Sensors, 10, 5590-5603.

Li, R.C.W., Ventura, L., Gruber, J., Kawano, Y., and Carvalho, L.R.F. (2008) A selective conductive polymer-based sensor for volatile halogenated organic compound (VHOC). Sensors and Actuators B: Chemical, 131, 646-651.

Li, X. and Dutta, P.K. (2010) Interaction of dimethylmethylphosphate with zeolite Y: impedance-based sensor for detecting nerve agent simulants. Journal of Physical Chemistry C, 114, 7986-7994.

Martins, A.V.G., Berlier, G., Bisio, C., Coluccia, S., Pastore, H.O., and Marchese, L. (2008) Quantification of bronsed sites in microporous catalysts by a combined FTIR and NH_3-TPD study. Journal of Physical Chemistry C, 112, 7139-7120.

McKeen, J.C., and Davis, M.E. (2009) Conductivity of mo-and divalent cation in the microporous zincosilicate VPI9. Journal of Physical Chemistry C, 113, 9870-9877.

Montserral, V., Joaquin, C., Albert. C., Albert, C., Ramon, M.J., and Jesus, S. (2007) Gas detection with SnO_2 sensors modified by zeolite films. Sensors and Actuators B: Chemical, 124, 99-110.

Mori, M., Nishimura, H., Itagaki, Y., and Sadaoka, Y. (2009) Potentiometric VOC detection in air using 8YSZ-based oxygen sensor modified with $SmFeO_3$ catalytic layer. Sensors and Actuators B: Chemical, 142, 141-146.

Panov, A.G. and Fripiat, J.J. (1998) An infared study of acetone and mesityl oxide adsorption on acid catalyst. Langmuir, 14, 3788-3796.

Ruangchuay, L., Sirivat, A., and Schwank, J. (2004) Electrical conductivity response of polypyrrole to acetone vapor: effect of dopant anions and interaction mechanisms. Synthetic Metals, 140, 15-21.

Ruangchuay, L., Sirivat, A., and Schwank, J. (2004) Selective conductivity response of polypyrrole-based sensor on flammable chemicals. Reactive and Functional Polymers, 61, 11-22.

Soontornworajit, B., Wannatong, L., Hiamtup, P., Niamlang, S., Chotpattananont, D., Sirivat, A., and Schwank, J. (2007) Induced interaction between polypyrrole and SO_2 via molecular sieve 13X. Materials Science and Engineering: B, 15, 78-86.

Tang, Li., Li, Y., Xu, K., Hou, X., and Lv, Y. (2008) Sensitive and selective acetone sensor based on its cataluminescence from Nano-La_2O_3 Surface. Sensors and Actuators B: Chemical, 132, 243-249.

Thongchai, N., Kunanuruksapong, R., Niamlang, S., Wannatong, L., Sirivat, A., and Wongkasemjit, S. (2009) Interactions between CO and poly(p-phenylene vinylene) as induced by ion-exchanged zeolites. Materials, 2, 2259-2275.

Thuwachaosoan, K., Chottananont, D., Sirivat, A., Rujiravanit, R., and Schwank, J. (2007) Electrical conductivity responses and interactions of poly(3-thiopheneacetic acid)/zeolites L, mordenite, beta, and H_2. Materials Science and Engineering: B, 140, 23-30.

Varsani, P., Afonja, A., Williams, D.E., Parkin, I.P., and Binions, R. (2011) Zeolite-modified WO_3 gas sensors-enhanced detection of NO_2. Sensors and Actuators B: Chemical, 160, 475-482.

Vijaya, J.J., Kenedy, L.J., Sekaran, G., Bayhan, M., and William, M. (2008) Preparation and VOC gas sensing properties of Sr(II)-added copper aluminate spinel composites. Sensors and Actuators B: Chemical, 134, 604-612.

Wannatong, L., Sirivat, A., and Schwank, J. (2008) Polypyrrole and its composites with 3A zeolite and polyamide 6 as sensors for four chemicals in lacquer thinner. Reactive and Functional Polymers, 68, 1646-1651.

Wessling, R.A. and Zimmerman, R.G. (1968) Polyelectrolytes from bis-sulfonium salts. U.S.Patent, 3, 401.

Yang, P., Ye, X., Lau, C., Li. Z., Liu, X., and Lu, J. (2007) Design of efficient zeolite sensor materials for n-hexane. Analytical Chemistry, 79, 1425-1432.

Yimlamai, I., Niamlang, S., Chanthaanont, P., Kunanuruksapong, R., Changkhamchom, S., and Sirivat, A. (2011) Electrical conductivity response and sensitivity of ZSM-5, Y, and mordenite zeolite towards ethanol vapor. Ionics, 17, 607-615.

Zhu, J.H, Ying, W., Yuan, C., and Wang, X.S. (1998) Dispersion of potassium nitrate and the resulting basicity on alumina and zeolite Y. Journal of the Chemical Society, Faraday Transactions, 94, 1163-1169.

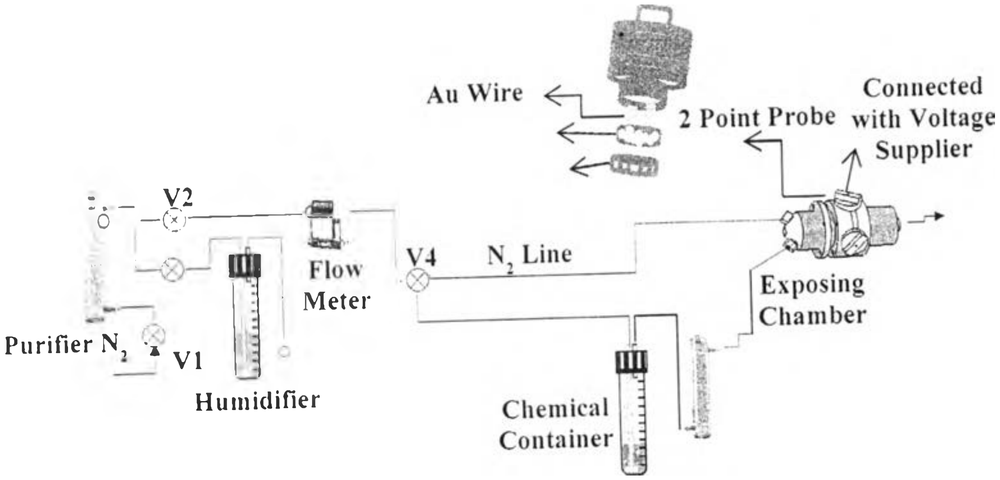

Figure 4.1 Schematic diagram of detection system.

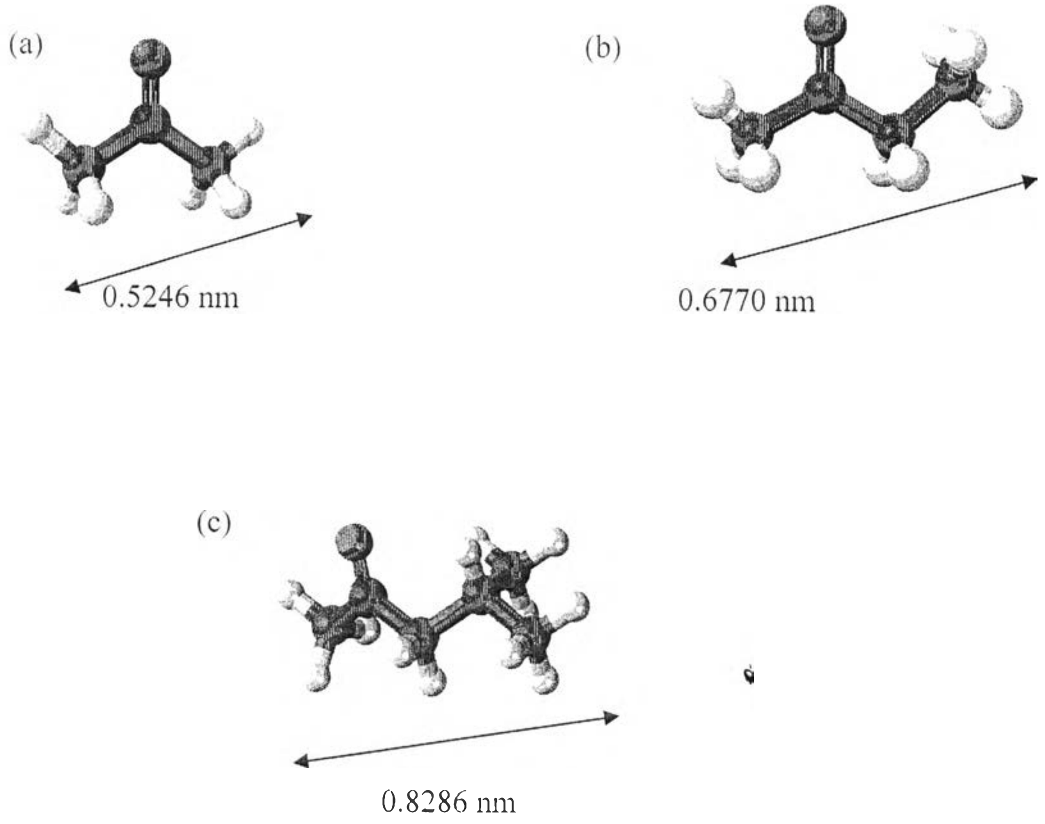

Figure 4.2 The molecular structures of: (a) Propanone (acetone); (b) Buta-2-one (MEK); and (c) 4-Methylpentan-2-one (MIBK).

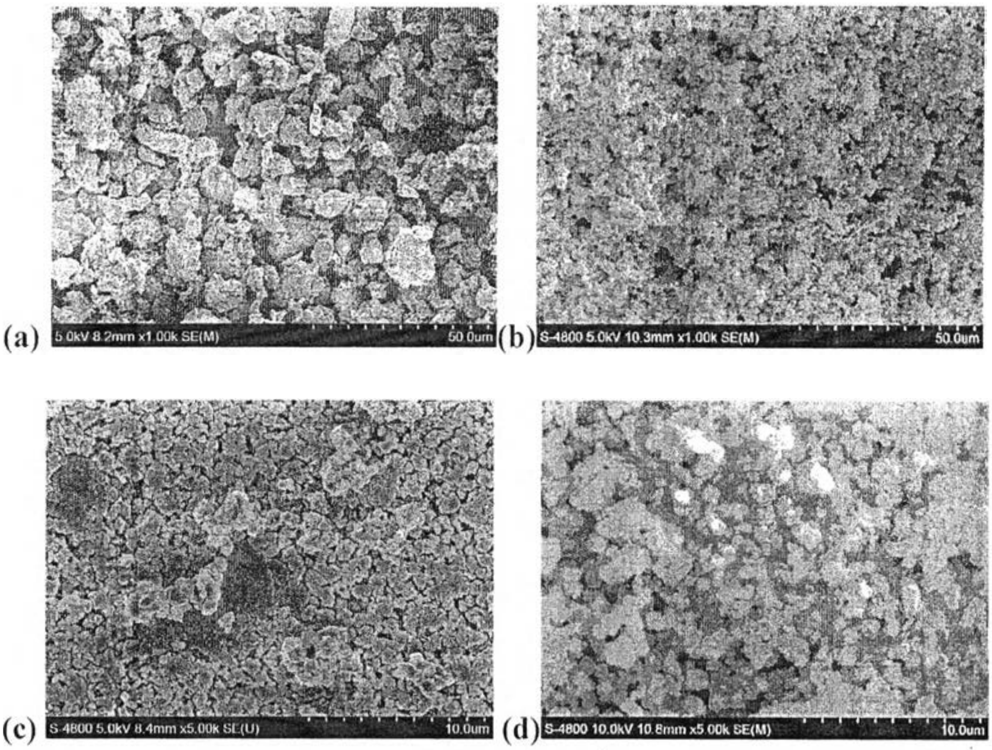

Figure 4.3 The morphology of dPPV powder, 80KNaY powders and, dPPV_[90]80KNaY pellet and powder at 10% v/v of dPPV: (a) dPPV at the magnification of 1000x; (b) 80KNaY at the magnification 1000x; (c) dPPV_[90] 80KNaY pellet at the magnification of 5000x; and (d) dPPV_[90] 80KNaY powder at the magnification of 5000x.

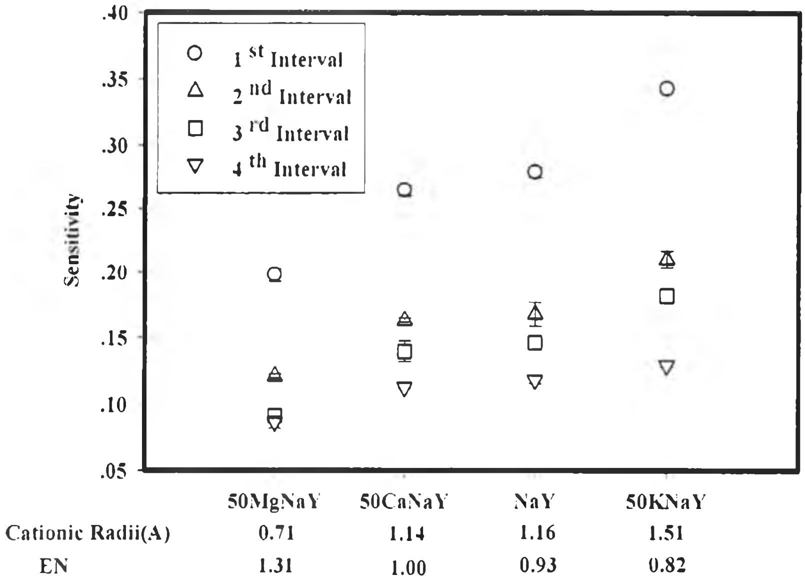

Figure 4.4 Sensitivity of the NaY, 50MgNaY, 50CaNaY, and 50KNaY in acetone exposure at 25 °C, 1 atm, at vapor concentration of 30000 ppm (3% v/v), and at the interval of 1200 sec.

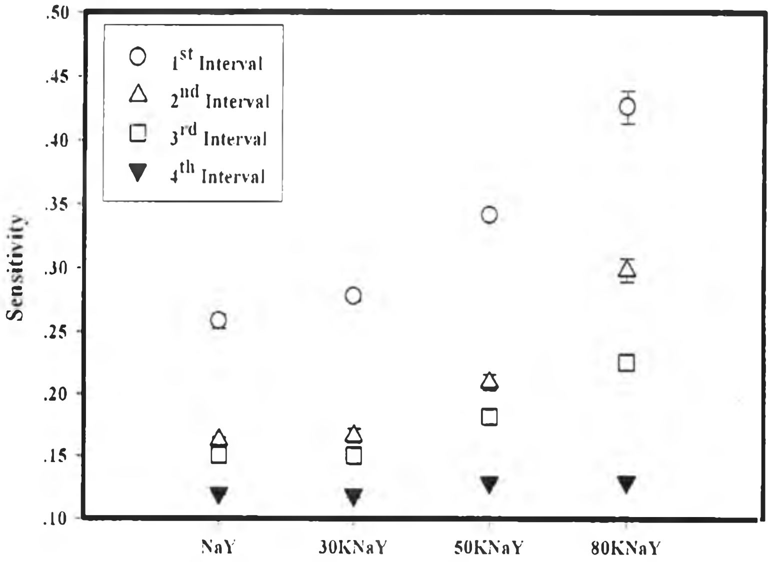

Figure 4.5 Sensitivity of the NaY, 30KNaY, 50KNaY, and 80KNaY in acetone exposure at 25 °C, 1 atm, at vapor concentration of 30000 ppm (3% v/v), and at the interval of 1200 sec.

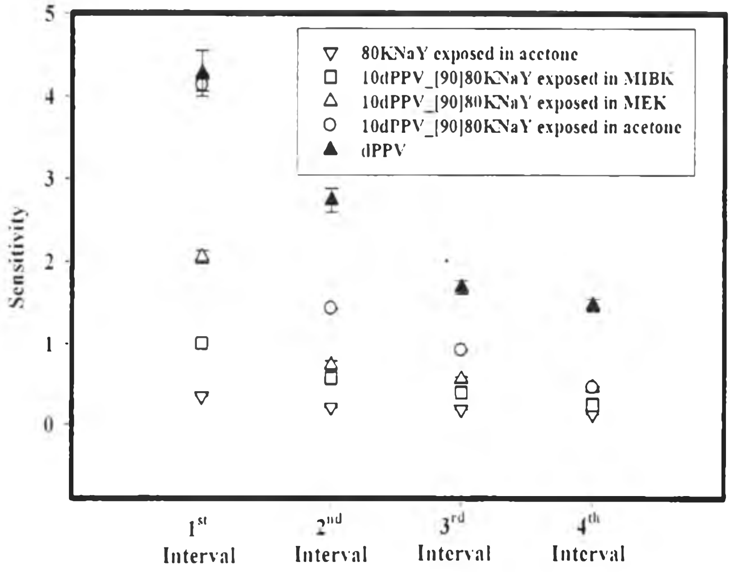

Figure 4.6 Sensitivity of the 80KNaY, dPPV_[90]80KNaY, and dPPV in acetone, MEK, and MIBK exposure at 25 °C, 1 atm, at vapor concentration of 30000 ppm (3% v/v), and at the interval of 1200 sec.

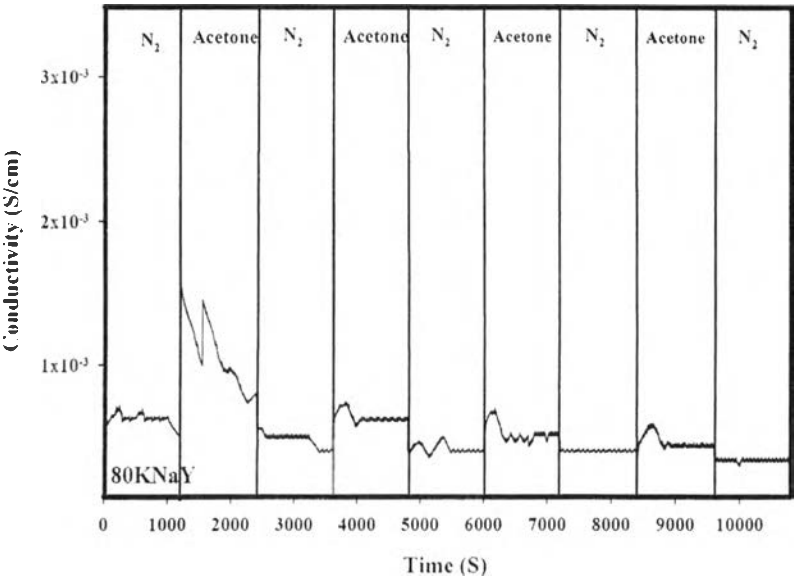

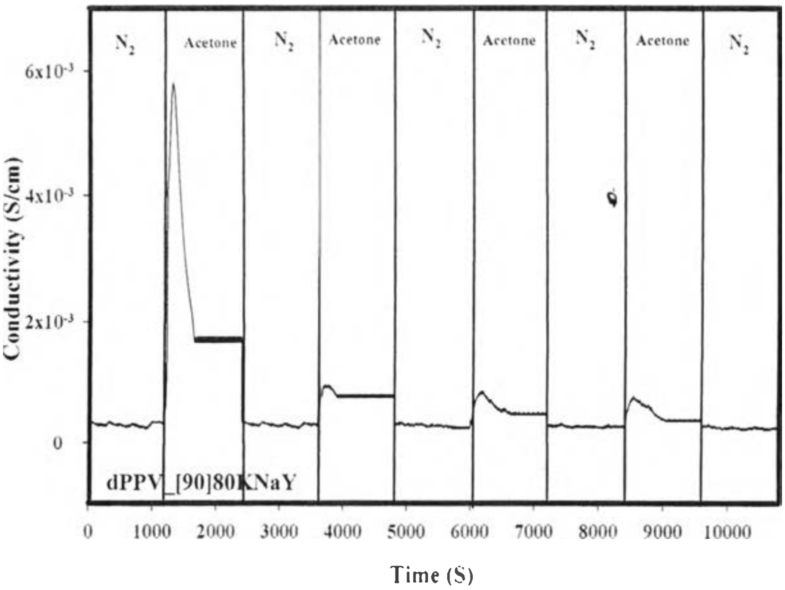

Figure 4.7 The cyclic responses of 80KNaY(top) and dPPV[90]80KNaY (bottom) during acetone exposure at the vapor concentration of 30000 ppm (3% v/v), and at the interval of 1200 sec.

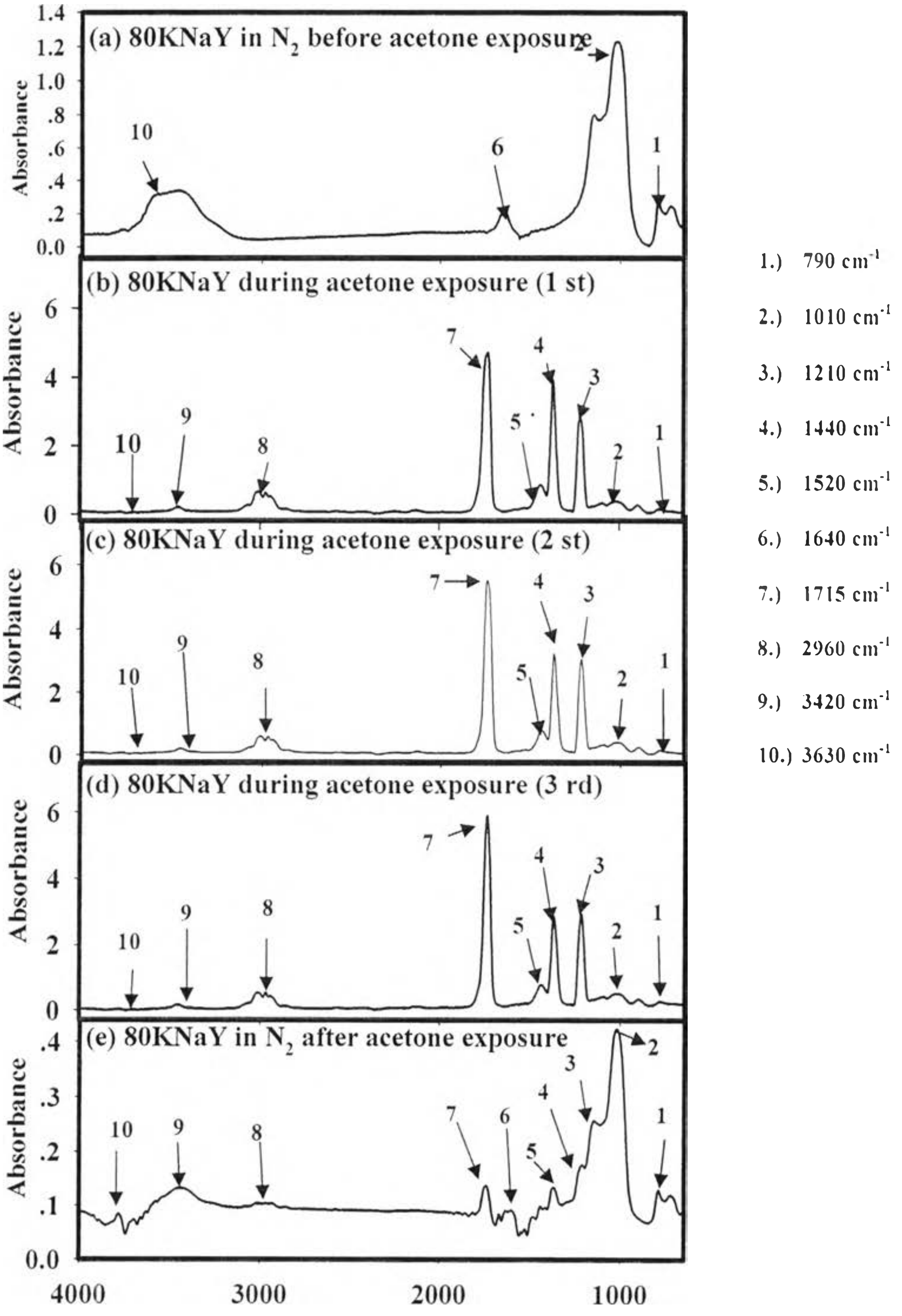

Figure 4.8 IR spectra of 80KNaY: (a) before acetone exposure; (b) acetone exposure 1st interval; (c) acetone exposure 2nd interval; (d) acetone exposure 3rd interval; and (e) after exposure at vapor concentration of 30000 ppm (pressure at 1 atm and at T=25°C).

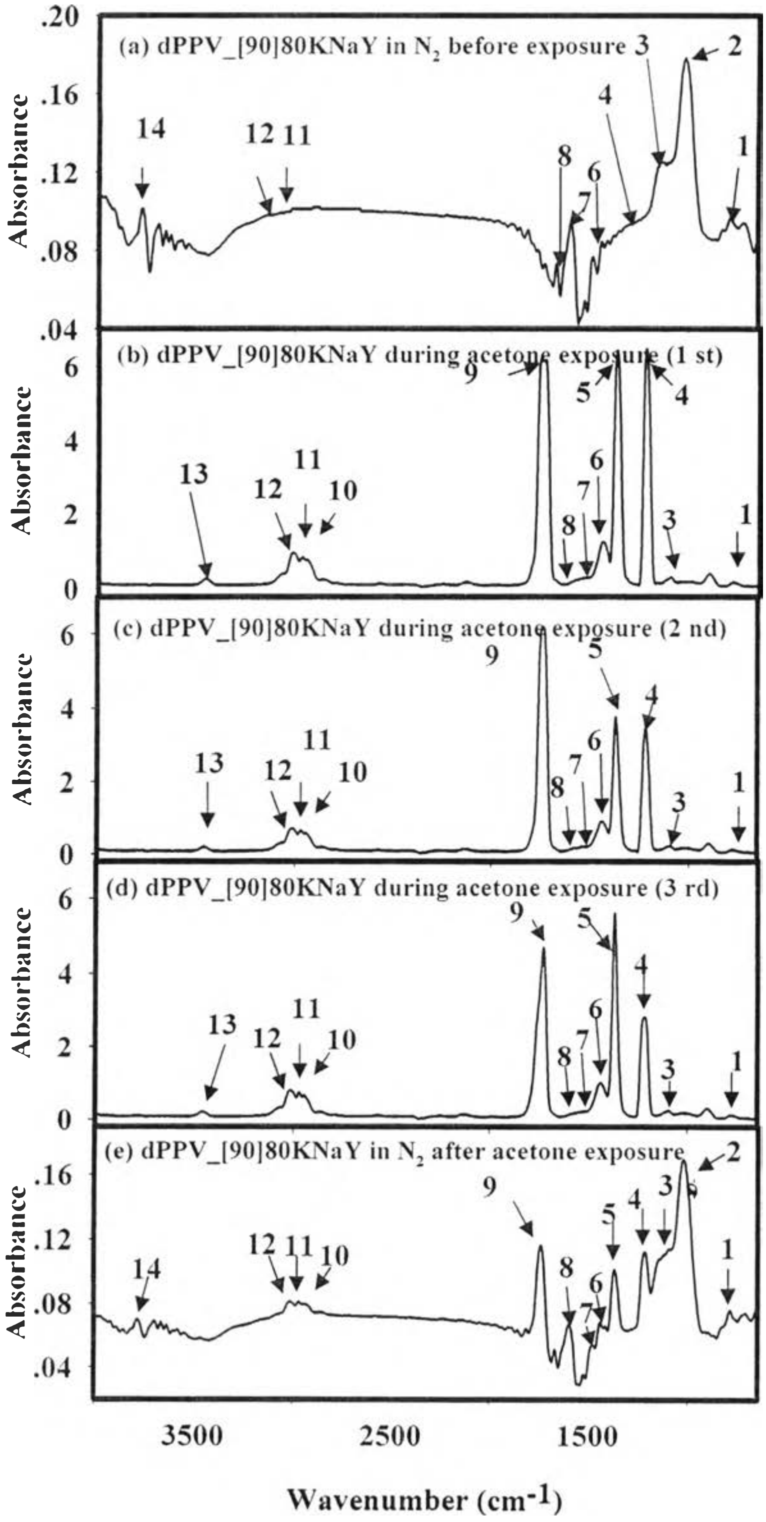

1.) 830 cm^{-1}
2.) 1010 cm^{-1}
3.) 1140 cm^{-1}
4.) 1210 cm^{-1}
5.) 1380 cm^{-1}
6.) 1440 cm^{-1}
7.) 1520 cm^{-1}
8.) 1620 cm^{-1}
9.) 1715 cm^{-1}
10.) 2820 cm^{-1}
11.) 2960 cm^{-1}
12.) 3022 cm^{-1}
13.) 3449 cm^{-1}
14.) 3630 cm^{-1}

Figure 4.9 IR spectra of dPPV_[90]80KNaY: (a) before acetone exposure; (b) acetone exposure 1st interval; (c) acetone exposure 2nd interval; (d) acetone exposure 3rd interval; and (e) after exposure at vapor concentration of 30000 ppm (pressure at 1 atm and at T=25°C).

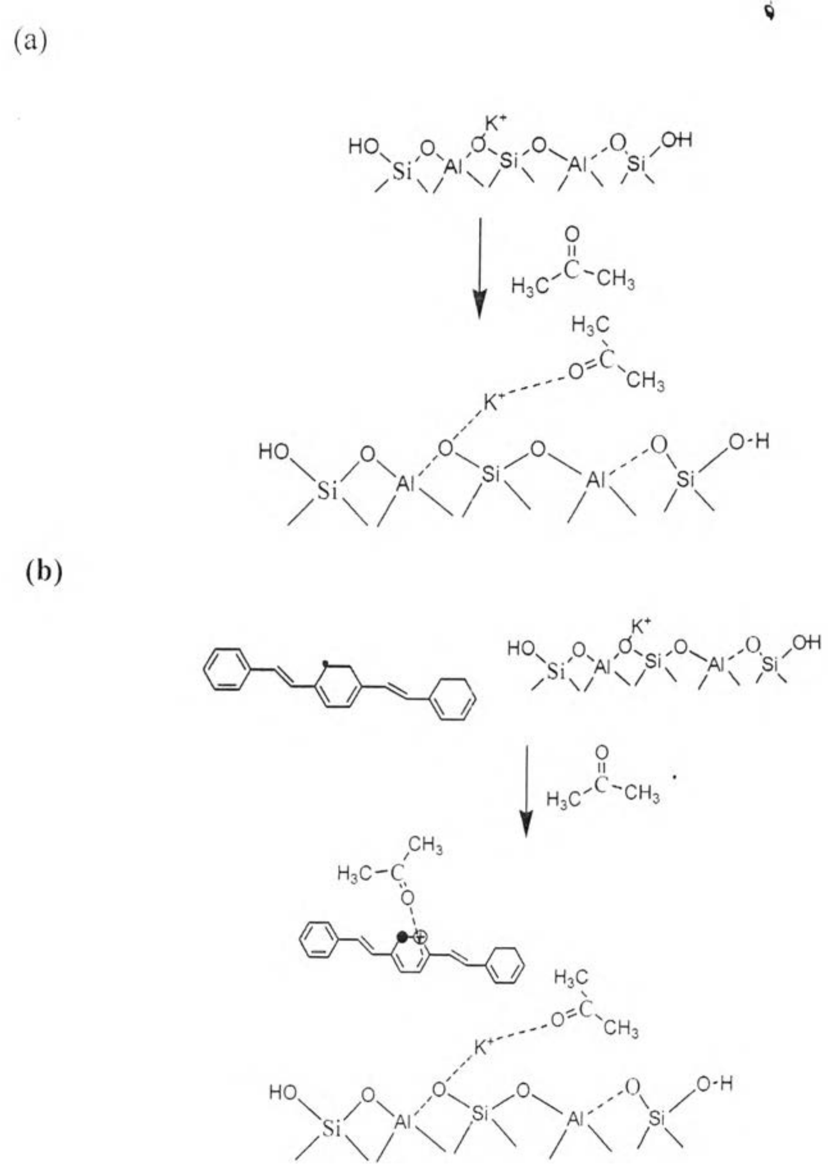

Figure 4.10 Proposed mechanism for the interactions of: (a) 80KNaY-acetone; and (b) dPPV_[90]80KNaY-acetone

Table 4.1 Structural, analytical data and electrical conductivity of dPPV, zeolite Y, and dPPV_zeolite Y

Sample	Sample Code	Zeolite Content (% v/v)	% mole of cation	EN	Ionic Radii (Å)	Median Pore Width (Å)	Surface Area (m^2/g)	σ_{air} (S/cm)	σ_{N2} (S/cm)
Doped poly(p-phenylene vinylene)	dPPV	0	-	-	-	-	-	$1.25\ x10^{1} \pm 7.30\ x10^{-1}$	$2.21\ x10^{-2} \pm 6.21\ x10^{-4}$
Zeolite Y (Si/Al=5.1and Na^{+})	NaY	100	100% Na^{+}	0.93 (Na^{+})	1.16 (Na^{+})	7.4875 ± 0.34	617.0 ± 7.0	$2.50\ x10^{-3} \pm 2.51\ x10^{-5}$	$8.38\ x10^{-4} \pm 2.27\ x10^{-5}$
Zeolite Y (Si/Al=5.1, Na^{+}, and Mg^{2+})	50MgNaY	100	53% Mg^{2+} and 47% Na^{+}	0.93 (Na^{+}) and 1.31 (Mg^{2+})	1.16 (Na^{+}) and 0.71 (Mg^{2+})	8.0750 ± 0.04	530.0 ± 2.0	$1.72\ x10^{-3} \pm 3.28\ x10^{-}5$	$3.73\ x10^{-4} \pm 3.71\ x10^{-6}$
Zeolite Y (Si/Al=5.1, Na^{+}, and Ca^{2+})	50CaNaY	100	55% Ca^{2+} and 45% Na^{+}	0.93 (Na^{+}) and 1.00 (Ca^{2+})	1.16 (Na^{+}) and 1.14 (Ca^{2+})	8.0600 ± 0.03	649.0 ± 6.0	$2.19\ x10^{-3} \pm 4.28\ x10^{-5}$	$7.69\ x10^{-4} \pm 3.70\ x10^{-6}$
Zeolite Y (Si/Al=5.1, Na^{+}, and K^{+})	50KNaY	100	56% K^{+} and 44% Na^{+}	0.93 (Na^{+}) and 0.82 (K^{+})	1.16 (Na^{+}) and 1.51 (K^{+})	7.7820 ± 0.39	553.0 ± 4.0	$5.55\ x10^{-3} \pm 5.27x\ 10^{-4}$	$1.06\ x10^{-3} \pm 2.27\ x10^{-4}$
10%v/v Doped poly(p-phenylenevinylene)_zeolite Y (Si/Al=5.1, Na^{+}, and K^{+})	dPPV_[90] 80KNaY	90	81% K^{+} and 19% Na^{+}	0.93 (Na^{+}) and 0.82 (K^{+})	1.16 (Na^{+}) and 1.51 (K^{+})	-	-	$1.12\ x10^{-1} \pm 3.58\ x10^{-2}$	$5.86\ x10^{-3} \pm 2.27\ x10^{-3}$

Table 4.2 Electrical conductivity sensitivity of dPPV, zeolite ,Y, and dPPV_zeolite Y exposed to acetone, MEK, and MIBK

Sample	Chemical Vapor	Electrical Conductivity Sensitivity			
		1st Interval	2nd Interval	3rd Interval	4th Interval
dPPV	acetone	$4.50 \pm 9.88 \times 10^{-01}$	$2.72 \pm 7.72 \times 10^{-01}$	$1.69 \pm 8.23 \times 10^{-02}$	$1.48 \pm 7.92 \times 10^{-02}$
NaY	acetone	$2.65 \times 10^{-01} \pm 1.89 \times 10^{-02}$	$1.68 \times 10^{-01} \pm 9.41 \times 10^{-02}$	$1.46 \times 10^{-01} \pm 2.75 \times 10^{-03}$	$1.18 \times 10^{-01} \pm 2.78 \times 10^{-03}$
50MgNaY	acetone	$1.97 \times 10^{-01} \pm 5.06 \times 10^{-03}$	$1.21 \times 10^{-01} \pm 1.42 \times 10^{-03}$	$9.12 \times 10^{-02} \pm 1.72 \times 10^{-04}$	$8.64 \times 10^{-02} \pm 4.22 \times 10^{-03}$
50CaNaY	acetone	$2.57 \times 10^{-01} \pm 2.40 \times 10^{-03}$	$1.63 \times 10^{-01} \pm 1.37 \times 10^{-02}$	$1.40 \times 10^{-01} \pm 8.21 \times 10^{-03}$	$1.12 \times 10^{-01} \pm 9.82 \times 10^{-42}$
30KNaY	acetone	$2.78 \times 10^{-01} \pm 4.42 \times 10^{-03}$	$1.68 \times 10^{-01} \pm 2.87 \times 10^{-03}$	$1.50 \times 10^{-01} \pm 1.58 \times 10^{-03}$	$1.18 \times 10^{-01} \pm 2.04 \times 10^{-03}$
50KNaY	acetone	$3.42 \times 10^{-01} \pm 4.67 \times 10^{-04}$	$2.09 \times 10^{-01} \pm 6.27 \times 10^{-03}$	$1.81 \times 10^{-01} \pm 6.12 \times 10^{-04}$	$1.28 \times 10^{-01} \pm 9.12 \times 10^{-04}$
80KNaY	acetone	$4.26 \times 10^{-01} \pm 1.25 \times 10^{-01}$	$2.92 \times 10^{-01} \pm 8.28 \times 10^{-03}$	$2.30 \times 10^{-01} \pm 4.40 \times 10^{-03}$	$1.30 \times 10^{-01} \pm 1.63 \times 10^{-03}$
dPPV_[90]80KNaY	acetone	$4.13 \pm 7.09 \times 10^{-02}$	$1.43 \pm 1.61 \times 10^{-02}$	$9.10 \times 10^{-01} \pm 6.98 \times 10^{-03}$	$5.27 \times 10^{-01} \pm 2.68 \times 10^{-03}$
dPPV_[90]80KNaY	MEK	$2.17 \pm 9.55 \times 10^{-02}$	$7.44 \times 10^{-01} \pm 4.29 \times 10^{-02}$	$5.48 \times 10^{-01} \pm 3.83 \times 10^{-02}$	$4.75 \times 10^{-01} \pm 1.10 \times 10^{-02}$
dPPV_[90]80KNaY	MIBK	$1.01 \pm 1.03 \times 10^{-02}$	$5.71 \times 10^{-01} \pm 2.98 \times 10^{-02}$	$3.89 \times 10^{-01} \pm 1.82 \times 10^{-02}$	$2.44 \times 10^{-01} \pm 3.16 \times 10^{-02}$